

Special Issue

Non-Destructive Testing and Assessment of Reinforced Concrete and Masonry Structures

In-situ and lab tests for mechanical characterization of stone masonry historical structures



António Arêde ^{a,*}, Celeste Almeida ^{a,b}, Cristina Costa ^{a,c}, Aníbal Costa ^d

^a CONSTRUCT-LESE, Faculty of Engineering (FEUP), University of Porto, R. Dr. Roberto Frias s/n, 4200-465 Porto, Portugal

^b Department of Civil Engineering, Faculty of Science and Technology, University Fernando Pessoa (UFP), Praça 9 de Abril 349, 4249-004 Porto, Portugal

^c Department of Engineering, Tomar School of Technology, Polytechnic Institute of Tomar, Quinta do Contador, 2300-313 Tomar, Portugal

^d RISCO, Department of Civil Engineering, University of Aveiro, Campus Universitário de Santiago, Aveiro 3810-193, Portugal

HIGHLIGHTS

- Experimental characterization of stone masonry joints made of as built materials.
- Stiffness parameters were obtained for both dry and mortar stone masonry joints.
- Bore-hole dilatometer and Menard pressuremeter tests on masonry infill material.
- Oedometric and triaxial test results were obtained for masonry infill material.
- Stiffness data for original infill material was made available for numerical models.

ARTICLE INFO

Article history:

Received 27 February 2018

Received in revised form 1 April 2019

Accepted 3 June 2019

Available online 12 June 2019

Keywords:

Stone masonry
Historical structures
Masonry interface joints
Masonry infill material
In-situ and lab testing
Borehole dilatometer
Ménard pressuremeter

ABSTRACT

The assessment of historical structures is a broad issue likely to comprise lab or in-situ testing at the structure, component or material levels, whenever relevant characterization of mechanical and physical properties is required. The material characterization of historical structures, particularly stone masonry ones as addressed herein, involve testing the constituent materials and their interfaces, namely stone blocks, interface joints (either dry or filled with mortar) and infill material. Besides stone, for which standard testing procedures are well established, interface joints and infill material testing are challenging issues. In such context, this paper reports a summary of the authors experience on characterizing materials, and respective interfaces, of historical constructions, aiming at providing input parameters' data for numerical simulations which are deemed useful for the scientific/technical community dealing with analysis of historical structures. The main focus of the paper is on stone masonry joints' testing and on infill material characterization by in-situ or lab tests. The reported experimental activities (e.g. borehole drilling and core sampling) can be considered as minor intrusive/destructive for the global constructions, because they are very localized and can easily repairable.

© 2019 Elsevier Ltd. All rights reserved.

1. Introduction

Conservation, maintenance and retrofitting of existing structures, in general, are well-established matters of concern throughout world-wide technical and scientific community. Environmental sustainability is dictating this endeavor in order to counterbalance strong trends for new construction in emerging

economy countries and wealthy societies where heritage constructions are not so present or dominant.

For the particular case of historical structures, although environmental issues are also important, other concerns take the lead, namely the respect for the existing heritage, relating to whole constructions, systems, elements, materials and techniques involved in past building procedures.

Therefore, interventions (or simply non-interventions) on built heritage, be it of culturally renowned historical value constructions or more modest traditional/vernacular building, should always be object of careful and comprehensive assessment to support the

* Corresponding author.

E-mail addresses: aarede@fe.up.pt (A. Arêde), celestea@ufp.edu.pt (C. Almeida), c.costa@ipt.pt (C. Costa), agc@ua.pt (A. Costa).

decisions on the need for intervention and, where necessary, for the most appropriate type complying with the widely and repeatedly stated compatibility and reversibility requirements [13].

Structural assessment, however, is a wide spectrum activity, likely to involve several and different types of complementary requirements. These can be synthetically summarized and ordered as: i) preliminary tasks (in-situ surveys, geometrical characterization, historical investigations, etc.); ii) diagnosis of existing and observed/suspected damage, looking for respective possible causes; iii) experimental activities, by lab or in-situ testing at the structure, components' or materials' levels, for relevant mechanical and physical characterization; iv) structural and physical monitoring (to find out or confirm effectively developing or stabilized damage, previously evidenced by visual inspections); v) numerical simulations of the structural response under relevant and pertinent loading conditions; vi) establishment of practically applicable, yet adequate and reliable, safety format framework appropriate for historical constructions (clearly an open and highly challenging issue on safety assessment); vii) safety verifications and decision on intervention options.

Each of the above mentioned tasks/requirements encompasses more or less complicated challenges, among which the mechanical and physical characterization by lab or in-situ testing at the structure, components' or materials' levels, is a key issue addressed in this paper. In particular, experience and practical application of different techniques for characterizing the material components of stone masonry constructions, namely stone, mortar and/or dry joints and infill materials (wherever they are present) was taken as the main focus of the paper. For that purpose, a few historical structures are referred as cases studied by the authors since 2000, wherein several material characterization testing techniques were adopted to provide some useful realistic data not yet published at international level. The addressed experimental activities are not strictly non-destructive, but still they can be considered as minor intrusive for the global constructions because interventions are very localized and easily erased/repared (such as borehole drilling and core sampling).

2. Material characterization of historical structures

2.1. General comments and previous works

The material characterization of historical structures, particularly stone masonry ones as addressed herein, involve testing the constituent materials and their interfaces. Materials typically consist of stone blocks (with more-or-less regular or irregular shapes), interface joints either dry or filled with mortar (poor lime-based mortar or a more consistent one including some contents of other hydraulic binder) and infill granular material.

Each material type can be tested stand alone, or combined. Typically, stone is normally characterized isolated without major difficulties. A few results of these are presented, relative to historical construction cases studied by the authors.

Concerning mortar, where it exists, it is not easy to perform tests on the isolated historic mortar material due to the obvious difficulties of extracting appropriate samples for testing, by contrast with new mortar for which standard tests (e.g. flexural and compression) are straightforward. However, the mortar characterization as an isolated material may not be of great interest since it seldom exists in real practice. In fact, it is more important to gather knowledge about mechanical (normal and tangential) behavior of stone-mortar joint assemblages, since these are much more representative of the existing reality. Tests on these conditions can be made in-situ or in lab on samples extracted from existing constructions or on reconstructed samples, for which, procedures and results are presented herein, stemming from cases studied by the authors.

Last but not the least, the infill material is important to be characterized by itself, either in-situ or in lab, resorting to samples taken from the real construction, as if it were a sort of soil, using soil mechanics testing techniques. In the following sections, in-situ and lab procedures are presented, as well as the corresponding results from the same case studies above mentioned.

Therefore, this paper contains a summary of the authors experience on characterizing materials (and respective interfaces) of historical constructions, providing a few results adopted in the numerical simulations and deemed useful for the scientific/technical community dealing with the analysis of historical structures. In brief, the main focus of the paper is on stone masonry joints' testing and on infill material characterization by in-situ or lab tests.

Concerning these issues, it is worth recalling existing experimental works reported in the literature, which, in fact appears very scarce.

Actually, for stone masonry joints' testing, to the authors' best knowledge, the oldest experimental study found is reported in the Portuguese publications LNEC [14] and Almeida [1], which in fact are works the present paper is based upon. From then on, very few other works addressed the topic: Vasconcelos [26] report an experimental study of stone masonry in shear and compression, but for new lab made specimens, focusing on the evaluation of shear and compressive mechanical properties under monotonic and cyclic loading, as well as the influence of the surface roughness and of the bed joint material on the masonry behavior. In the same line, Milosevic et al. [20] presents an experimental work on rubble stone masonry where cohesion and friction parameters were obtained by triplet tests. Subsequently, most of the works found are focused on clay brick masonry, almost all of them concerning tested and numerically studied lab made specimens, such as those reported in Domède et al. [11], Ghiassi et al. [12], Mazzotti et al. [18], Raham and Ueda [24], Pavan et al. [21], Pelà et al. [22] and Sandoval and Arnau [25]. Amongst all the referred, despite relative to clay brick masonry, only the work reported in Pelà et al. [22] is in line with the present paper research and tends to confirm the utility and validity of testing core-drilled samples of masonry joints.

Also, concerning infill material characterization by in-situ testing, very few works were found. Despite focused in foundation elements, it is worth referring the work by Macchi et al. [17] about the Leaning Tower of Pisa, in which borehole dilatometers were used for testing the characteristics of the foundation ring in order to check the conditions of previous strengthening by grouting. Afterwards, again to the authors' best knowledge, only in 2000, the Portuguese publications LNEC [14] and Almeida [1] addressed the use of borehole dilatometer tests (normally used for rock mechanics) to characterize the deformability of infill material of ancient and massive masonry thick walls. From then on, only the work of Lombillo et al. [15] mentions hole-drilling and dilatometer tests on rubble stone masonry structures (providing test description without results and with an application in laboratory) and, later on, Lombillo et al. [16] applied hole-drilling and mini-pressurimeter (similar to dilatometer) for evaluating the mechanical characteristics of a rammed earth wall built and tested in lab. More recently, in line with the authors' experience related with dilatometer testing, new applications were made as described in Arède et al. [4] and Mesquita et al. [19], similar to those reported in LNEC [14] and Almeida [1], though with a Ménard pressurimeter.

Based on the exposed, it is apparent that very little attention has been given by researchers to the experimental characterization of existing old stone masonry, particularly in terms of joint and infill material minor destructive testing using hole-drilling coupled with in-situ dilatometer tests and lab tests on extracted samples. Since realistic material data is crucial for obtaining credible numerical simulations of ancient stone masonry heritage, it becomes clear the pertinence of the topics addressed in the following.

2.2. Masonry constructions object of experimental characterization

A few constructions, thoroughly studied, have provided conditions and material samples for the above mentioned tests. Their main characteristics are briefly described next for completeness.

The first is the “Serra do Pilar” monastery church, founded back in 1537, located in Vila Nova de Gaia, adjacent to the south bank of Douro river and facing the historical center of Porto, Portugal. The initially existing church was later replaced by a new, larger and cylindrical one, finished in 1678. Made of local granite stone, probably inspired in the Rome Pantheon as shown in Fig. 1, it was an innovative option contrasting with the dominant Portuguese architecture by that time. The church is 29.6 m high with external radius around 15 m (Fig. 1-a)), covered by a 0.60 m thick hemispherical dome with 23.0 m internal diameter, above which 4.0 m high columns (separated by windows) support another small dome (Fig. 1-b)) completing the roof structure (Fig. 1-c)). The church structure has eight buttresses (16.8 m high) between small chapels (Fig. 1-d)) defined by arches which provide support to windows. In the main chapel zone there is a larger arch (13.4 m high) adjacent to a 14 m high vault covering the main altar which develops along a rectangular shape zone.

Besides dynamic identification tests described in Almeida [2] that allowed calibrating the global structure stiffness by comparison with finite element numerical modelling, other experimental activities were made, namely core sampling to perform in lab material tests (on stone and joints) and borehole dilatometer (BHD) in-situ testing as described latter.

The second and third cases refer, respectively, to the D. Zameiro and Lagoncinha bridges, both located not far from Porto and crossing the same Ave river, with similar construction dates and

features. Fig. 2-a shows an overall view of D. Zameiro bridge that suffered partial collapse of a pier (Fig. 2-b) from which infill material samples were taken for lab characterization.

Fig. 3 shows a general old view (a) and a partial recent picture (b) of the Lagoncinha bridge that in late 1990’s was found with several damages in some arches due to traffic and foundation settlement. From this bridge only stone material samples (Fig. 3-c and -d) were extracted for lab characterization; due to the poor conditions of the samples, joint tests could not be made. More details about this bridge and a corresponding comprehensive study (including detailed numerical simulations) can be found in Costa [7].

The fourth and last case, generally illustrated in Fig. 4-a), is the “new” Vila Fria bridge, built between 2003 and 2005, to replace an old passage over the Vizela river about 60 km from Porto.

Being a newly built construction, all materials, elements and the whole bridge were thoroughly studied and characterized as detailed in Costa [8,9], Costa et al. [9,8] and Costa [10]. Besides material testing, the bridge was instrumented with a large monitoring system, Arêde et al. [3], subjected to a load test and object of a broad/detailed numerical study, Costa [10], calibrated with properties taken from material tests, some of which are reported hereafter.

3. Material characterization of historical structures

3.1. Stone lab testing

Mechanical and physical characterization of the granite stone can be carried out according to current standard tests, namely:

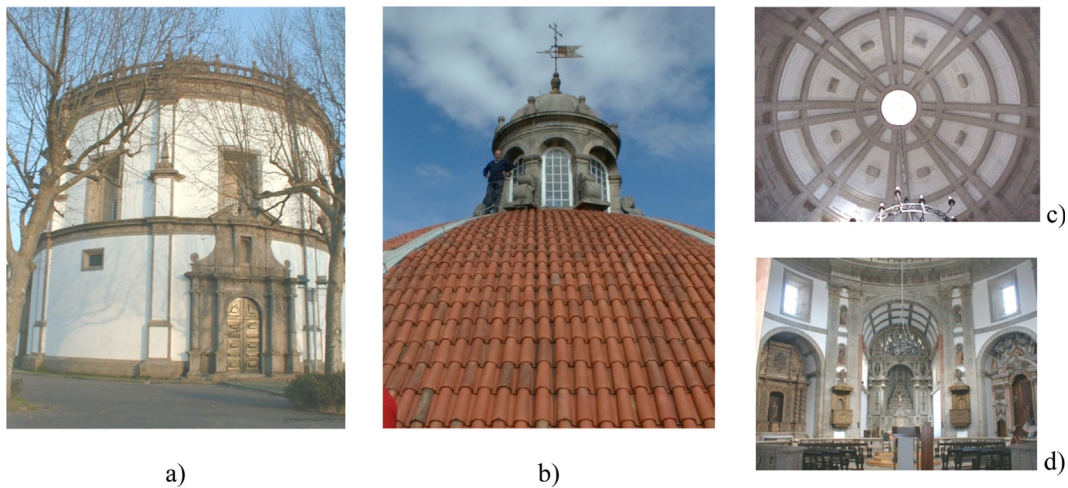


Fig. 1. The “Serra do Pilar” monastery church: a) Outside, b) the roof and the small upper dome, c) the dome structure and d) inside.



Fig. 2. D. Zameiro bridge: a) general view, b) partially collapsed pier.

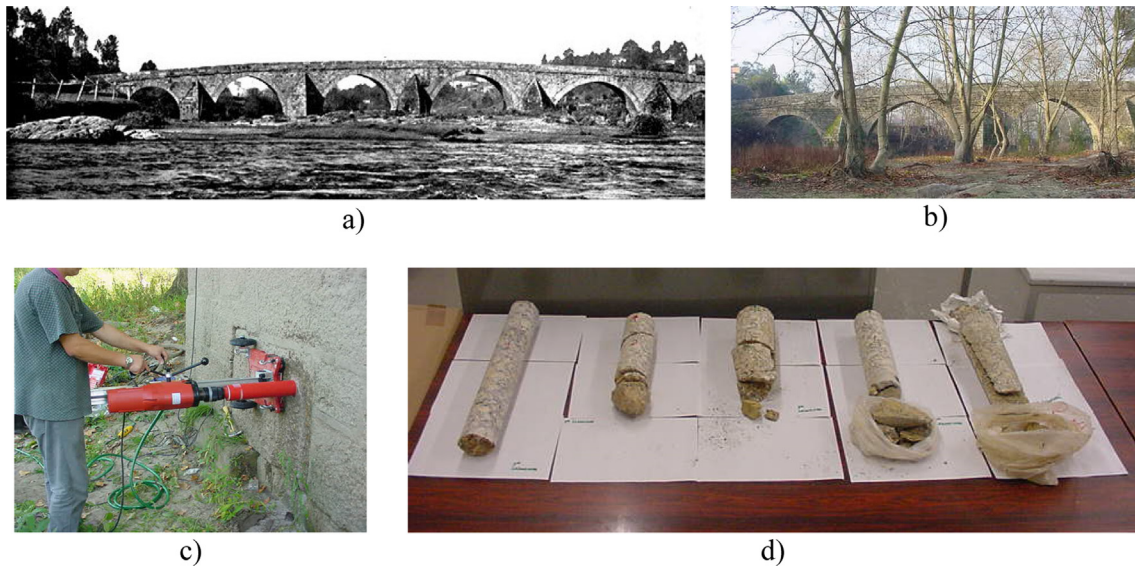


Fig. 3. Lagoncinha bridge: a) general old view, b) partial upstream view, c) core sampling and d) obtained samples.

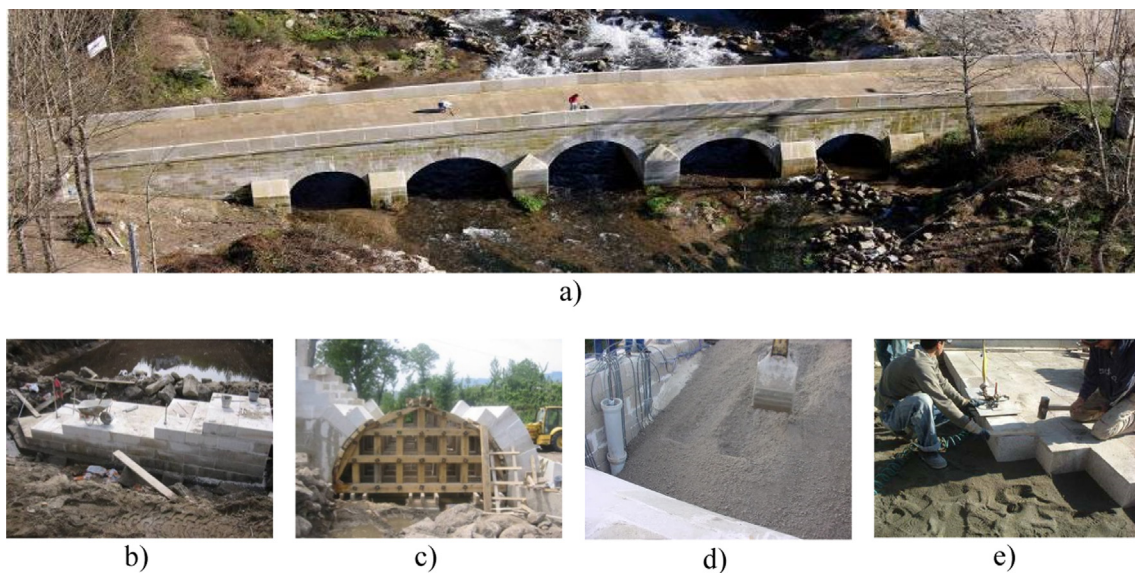


Fig. 4. New Vila-Fria bridge. a) General aerial view (courtesy of Prof. Francisco Piqueiro, FEUP) and constructive phases: b) piers, c) arches, d) infill and e) pavement.

uniaxial compressive strength; splitting tensile strength by diametral compression; compressive deformability Young modulus; natural stone porosity and water absorption coefficient. These tests are based on well established procedures for which further comments are not worth referring herein. For three of the case studies above presented, some of the obtained physical/mechanical properties are reported in Table 1 in terms of average values and variation coefficients, just for reference purposes. Compression strength of granite stone of Vila Fria bridge was evaluated on both dry and saturated specimens, as also included in the same table. Values are typical of granite stone, with variations attributable to different stone origins and weathering processes, for which further comments are deemed unnecessary herein.

3.2. Interface joints' lab testing

When dealing with stone masonry constructions involving stone, mortar and/or infill material (generally granular), joints

can be of different types according to the interface, namely: stone-to-stone dry joints (with no mortar); stone-to-stone mortar joints and stone-to-infill joints. All these types are addressed in the following, reporting experimental results obtained concerning shear and normal compression behavior. Case studies which provided these results are the Serra do Pilar church and the Vila Fria bridge.

3.2.1. Characterization of masonry joints of the Serra do Pilar church

From the Serra do Pilar church case, original mortar and dry stone-to-stone joints were made available by staff of FEUP labs and tests were carried out at LNEC (National Laboratory of Civil Engineering, Lisbon, Portugal), as reported in LNEC [14] and Almeida [1]. The mortar joints were prepared from large diameter (150 mm) sample cores drilled from the church walls. The dry joints were also conditioned in the lab to ensure surface finishing similar to that of masonry blocks.

Table 1
Physical and mechanical parameters of granite stone blocks.

Material parameter		Average values		(Coef. Variation)		Standard	
		Vila Fria bridge		Lagoncinha bridge		Serra do Pilar	
Compressive strength	(MPa)	66.9	(9%)	51.0	(26%)-	95.0-	(3%)
		32.4 ⁽¹⁾	(28%)				
Tensile splitting strength	(MPa)	3.7	(15%)	5.4	(34%)	3.5 ⁽²⁾	(-)
Young modulus	(GPa)	22.4	(27%)	39.2	(46%)	20.8	(19%)
Unit weight	(kN/m ³)	24.1	(1%)	26.4	(1%)	25.9	(9%)
		24.5 ⁽¹⁾	(1%)				
Porosity	(%)	4.0	(4%)	-		-	
Water absorption	(g/m ² /s ^{0.5})	36.7	(8%)	-		-	

⁽¹⁾ Saturated specimens.

⁽²⁾ Only one sample.



a)



b)

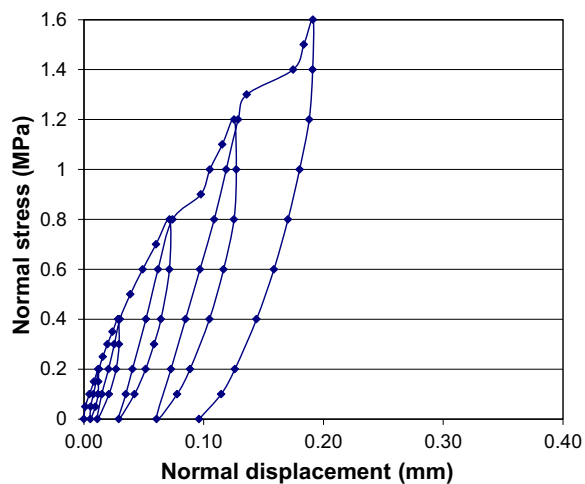
Fig. 5. Sample of mortar joint: a) ready for testing; b) after test.

Both shear and normal tests were made in the same shear-box machine existing at LNEC, with internal dimensions of $200 \times 200 \text{ mm}^2$. Therefore, the joints were encapsulated by a concrete envelope with adequate shape to fit inside the shear-box as shown in Fig. 5, with the surface to be sheared placed horizontally and along the shearing plane. In total, 11 mortar joints and 8 dry joints were tested.

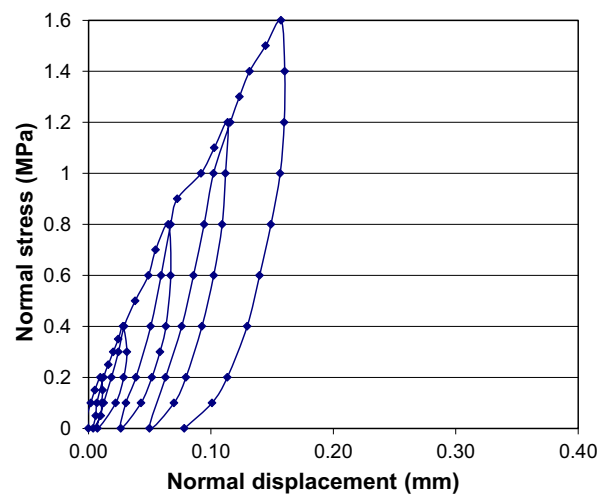
Before the shear tests, normal compression loading-unloading tests were made, comprising 5 cycles for increasing stress steps up to 1.6 MPa, on both mortar and dry joints. The results were plotted in normal stress vs normal displacement diagrams, which allowed extracting behavior parameters, namely normal stiffness

values for loading ($k_{n,l}$), i.e., first loading up to a given “virgin” stress level and for reloading phases ($k_{n,r}$). These parameters are often very important and useful for detailed numerical simulation models of stone masonry. Results were averaged across the whole set of tested samples of the same type.

Examples of normal compression test plots of mortar and dry joints are shown in Fig. 6. The former (Fig. 6-a) exhibits larger deformability for first loading than for reloading and also shows some sudden increases of normal displacement due to mortar crushing that was audible during the test. The dry joint plot (Fig. 6-b) shows similar trend in terms of deformability, but not the sudden increases of displacement.



a)



b)

Fig. 6. Examples of normal stress vs normal displacement plots: a) mortar and b) dry joints.

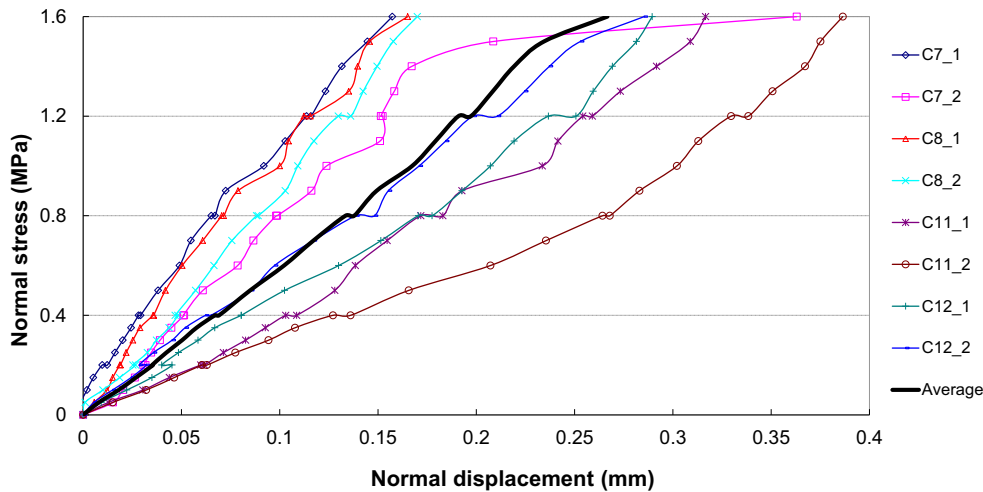


Fig. 7. Normal stress tests' plots and average curve, of first loading branches of dry joints.

The first loading branches (of the same joint type) were separated Almeida [1] from the unloading/reloading branches and plotted together for all tests as shown in Fig. 7 for the dry joints; these curves correspond to the envelope curves from the cyclic tests. For each stress level, the displacements were averaged, leading to the thick black line for which a linear approximation led to the value 6.24 MPa/mm for normal loading stiffness $k_{n,l}$.

For the normal reloading stiffness ($k_{n,r}$) of dry joints, values are roughly twice as that above referred. According to [14], mortar joints exhibited values of normal stiffness of the same order of those of dry joints, though slightly lower.

Similarly, shear tests were made for a set of increasing normal stress levels, both for dry and mortar joints. Since for the latter, joint halves were not separated, the shear test started by initial shearing of the sample leading to the mortar rupture and sample splitting into two halves. Four normal stress levels were applied (0, 0.2, 0.4 and 0.8 MPa) for these initial shearing tests of different joints and the results were plotted in shear stress vs. tangential displacement plots (Fig. 8) characterizing the first-shear response.

By averaging the shear tests' results as above explained, the four curves shown in Fig. 8-a) were obtained for mortar joints corresponding to the four normal stress levels. After split and replaced

in the original position, each mortar joint was sheared again under increasing normal stresses of 0.2, 0.4 and 0.8 MPa, with due care of removing loose mortar residuals caused by joint wear during each previous shear. These second phase tests are called sliding tests, with the corresponding average results shown in dashed-line curves plotted in Fig. 8-b) together with the solid line average curves relative to the respective shear tests. The comparison of these two types of curves, the so-called shear and sliding curves, shows that once the peak strength in shear curves is overcome the response tends to a residual stress plateau slightly above the maximum stress reached in sliding tests, as expected considering the adopted test sequence. Fig. 8-b) also evidences the expected effect of the compression on both the shear and the sliding response, traduced by the increase of strength and stiffness for higher compression levels. For the highest compression level, the difference of peak and residual shear strength is quite apparent, as commonly observed in materials following a Mohr-Coulomb type behavior.

It is worth commenting that average curves were preferred rather than envelope curves in order to provide mean trends of stress-displacement relationships which are generally adopted for numerical simulations. Should the analysis purpose be differ-

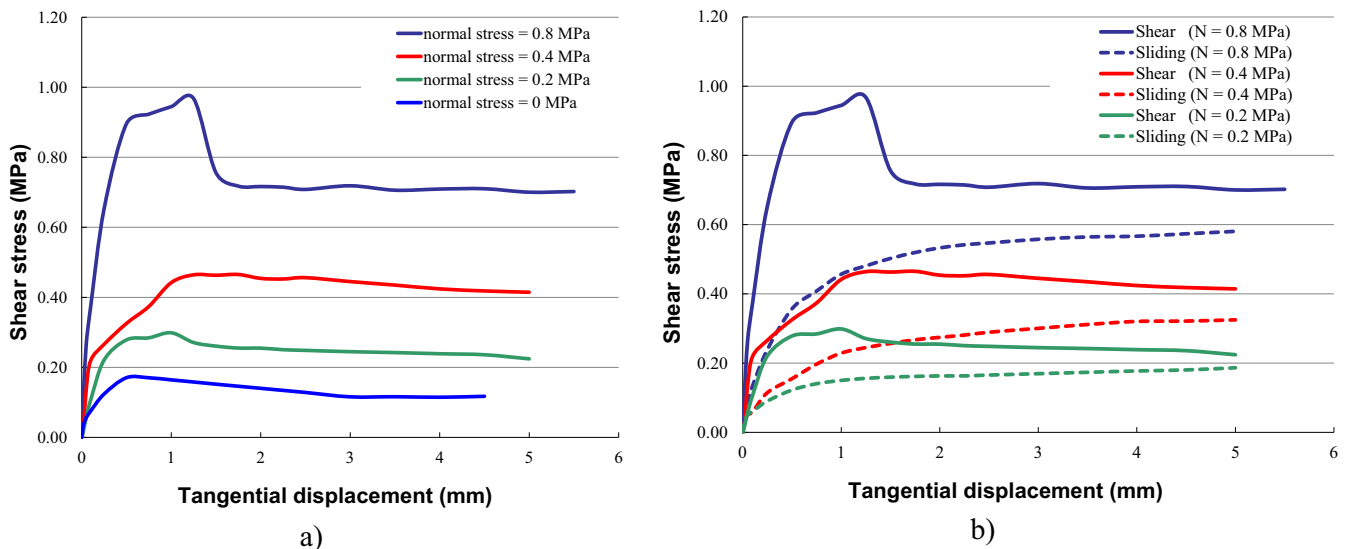


Fig. 8. Average shear stress - displacement curves of mortar joints: a) first shear tests and b) sliding tests compared with first shear tests.

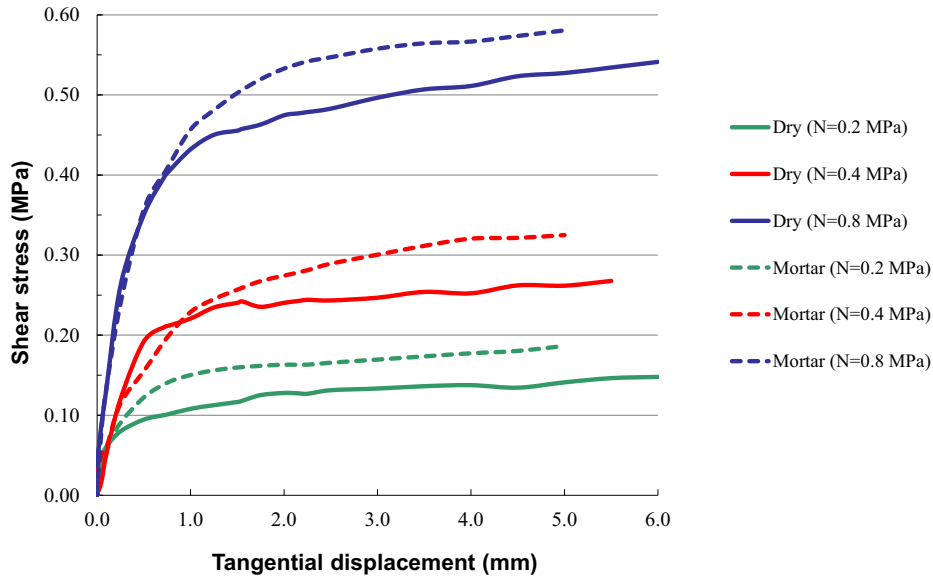


Fig. 9. Comparison of average shear stress - shear displacement curves from sliding tests of mortar joints (dashed lines) and dry joints (solid lines).

ent, e.g. safety assessment, other curve types (envelopes or some kind of “characteristic values” curve) could be easily derived and adopted.

A similar study was made for dry joints and comparison with average shear curves of mortar joints can be observed in the plots shown in Fig. 9, where solid lines refer to dry joint curves and dashed ones to the mortar joints sliding shear response. Despite showing similar initial stiffness, the mortar joints reach larger shear strength, probably resulting from better connection provided by the mortar material.

For a comprehensive presentation and interpretation of results, average curves obtained from normal compression and sliding tests were plotted in a combined diagram shown in Fig. 10 (for the dry joints case) which, simultaneously, evidences the shear response curves for different pre-compression levels, the normal compressive response (namely the normal stiffness in terms of first loading, $k_{n,l} = 6.24 \text{ MPa/mm}$) and the Mohr-Coulomb line ($\phi = 35.6^\circ$) adjusted to the pair of values of maximum shear strength and associated compression level.

3.2.2. Characterization of masonry joints of the Vila Fria bridge

From the Vila Fria bridge case, both stone-to-stone dry and new mortar joints, as well as stone-to-infill joints were prepared and tested using rock mechanics specific equipment and compression testing machines available at FEUP civil engineering laboratories, as described in Costa [10]. Assemblages of materials representing (dry and mortar) stone-to-stone joints and stone-to-infill joints have been tested using samples of materials (granite stone, hydraulic mortar and graded granular material) used in the Vila Fria bridge construction.

For testing masonry joints, two granite-stone parallelepiped samples with $200 \times 200 \times 75 \text{ mm}^3$ dimensions were used; the contact between the two stones was set in the larger area faces. For mortar joints, stones were connected by a layer of hydraulic mortar equal to that used in the bridge construction and with similar thickness (about 7 mm), as shown in Fig. 11-a. The joints between the stone and infill material were characterized by testing samples of pure granular material used in the backfill and a stone block with dimensions equal to the blocks used in the above mentioned joint tests (see Fig. 11-c).

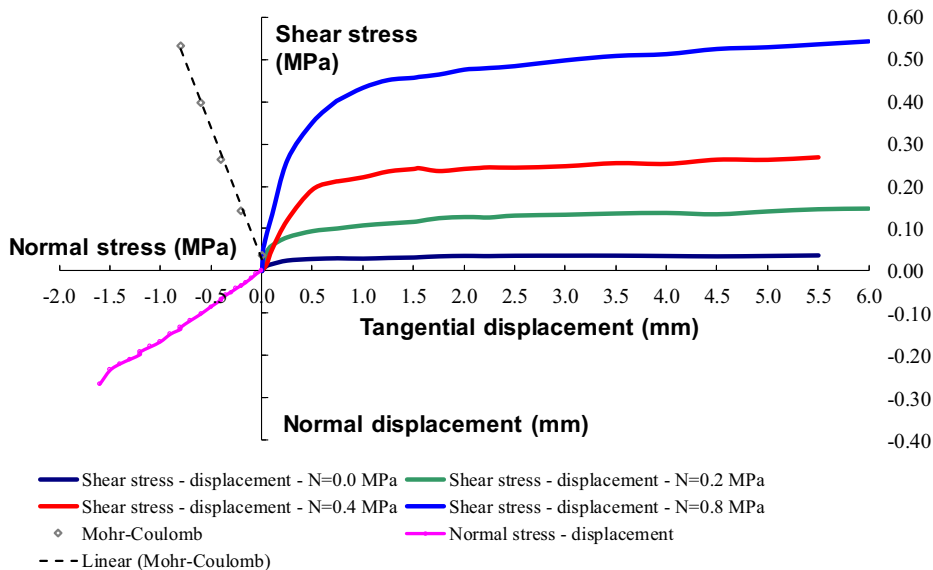


Fig. 10. Global average plots for dry joints: shear stress-displacement curves; normal stress-displacement response and adjusted Mohr-Coulomb line.

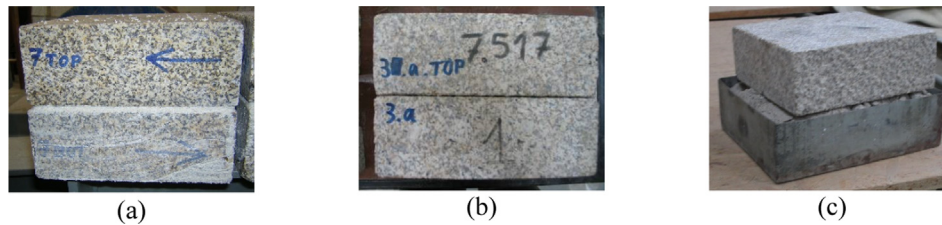


Fig. 11. Vila Fria bridge samples of: (a) stone-to-stone mortar joints, (b) stone-to-stone dry joints (c) and stone-to-infill joints.

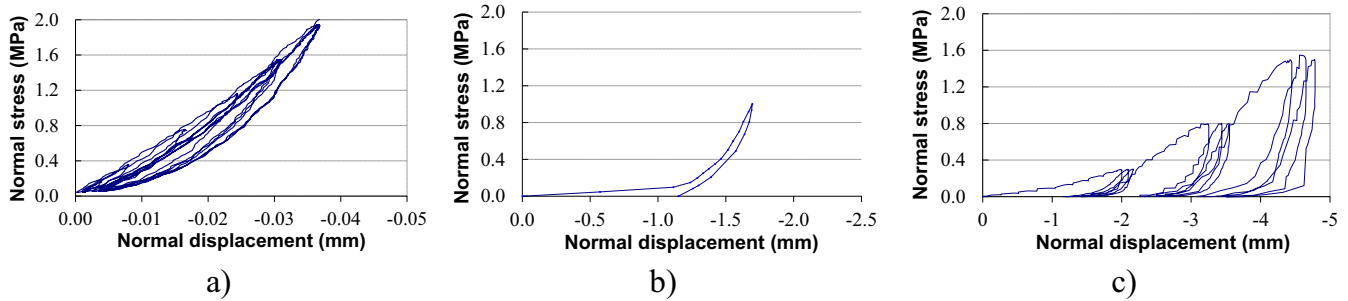


Fig. 12. Normal stress vs. vertical displacement of: (a) the stone-to-stone mortar joints, (b) stone-to-stone dry joints and (c) stone-to-infill joints.

The characterization of the joint behavior in the normal direction was based on the results of cyclic compression tests, which provided records of the evolution of compressive strength, σ , with the normal displacement, d , as shown in Fig. 12 for one example of each joint type.

For mortar stone-to-stone joints (6 tests performed) and stone-to-infill joints (just 1 sample tested) it was possible to evaluate the degradation of normal stiffness and compressive strength of joints due to successive cycles of loading-unloading-reloading. Mortar joints (Fig. 12-a) show loading branches characterized by roughly constant stiffness, k_{ni} , with an average value around 62 MPa/mm, about ten times that of the Serra do Pilar church. The unloading-reloading cycles showed positive curvature and, in general, strength recovery. Stone-to-stone dry joints (2 tests performed) and stone-to-infill joints (Fig. 12-b and -c) exhibit positive curvature in the first compression loading phases, with initial large deformability, characteristic of adjustments between joint surfaces, followed by considerable normal stiffness increase. For dry stone joints, such stiffness reached values about 1.2 to 2.8 MPa/mm, after the initial adjustment phase. Stone-to-infill joints show three loading branches with approximately constant stiffness of 0.1, 0.2 and 0.5 MPa/mm, about ten times lower than those of the Serra do Pilar dry or mortar joints. The unloading-reloading cycles also exhibit positive curvature, characterized by two branches of roughly constant stiffness with the transition between the two branches for both unloading and reloading phases occurring for similar stress levels. As usual, residual displacements are observed after unloading.

The tests for joints' shear behavior characterization were performed using 27 samples, of which 19 for mortar masonry joints, 5 for dry masonry joints and 3 for stone-to-infill joints considering different levels of the normal stress. Taking advantage as much as possible of the available material, some dry joint samples and all the stone-to-infill joints were subjected to more than one sliding test, although adopting conveniently spaced values of normal stress.

Each specimen was previously subjected to pre-compression, with different normal stress levels ranging from near zero to 1.2 MPa, aiming at covering a reasonable range of plausible values on the stone masonry elements.

The shear tests allowed identifying failure modes, shear strength evolutions vs. horizontal displacement for different normal stress levels, elastic shear stiffness values, Mohr-Coulomb envelope and evolutions of normal displacement vs. horizontal displacement.

The shear behavior of joints is expressed in terms of shear stress vs. horizontal displacement diagrams (τ , γ), under different levels of constant normal stress. Fig. 13 shows the (τ , γ) curves obtained for all mortar joints and all normal stress levels, after correcting the horizontal displacement as described in Costa [10]. In the same figure, thicker line curves are also included, which correspond to average curves adjusted to the set of curves obtained for each level of normal stress. These curves are typically characterized by a linear phase followed by softening and a residual phase. Although not shown herein, dry and stone-to-infill joints exhibit a linear branch followed by hardening and plateau phases; details can be found in Costa [10].

In these tests, generally it was found that the initial stiffness, the peak shear and the residual shear stress are higher, for larger levels of installed normal stress. For mortar joints the obtained stiffness values ranged between 0.12 and 0.76 MPa/mm; for dry

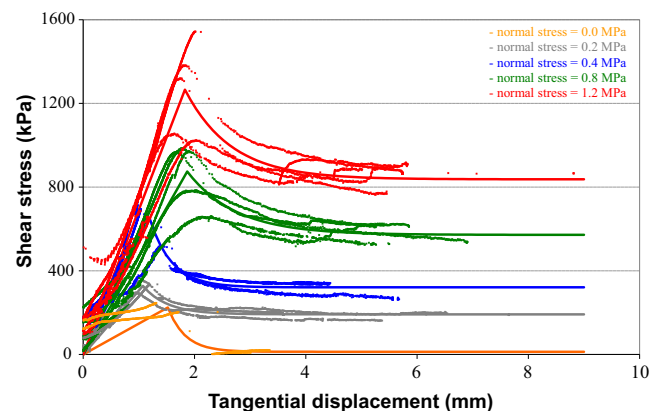


Fig. 13. Shear stress vs. tangential displacement of stone-to-stone mortar joints.

joints it ranged between 0.05 and 0.98 MPa/mm, while for stone-to-infill joints it falls in the interval 0.09–0.40 MPa/mm. It was also possible to verify that, in the normal direction of mortar joints, dilatancy was found in the pre-peak phase, followed by contraction after initiating the softening branch; the dry joints were found to remain dilatant until the plateau phase.

Regarding the strength parameters defining the Mohr-Coulomb failure envelope of the mortar joints, the friction angle and cohesion values were found about 41° and 210 kPa, respectively. Null cohesion was obtained for both the dry joints and the stone-to-infill joints, while friction angles were found as 30° and 27° , respectively.

A similar procedure, using the same equipment, was adopted later for the characterization of joints, under normal and shear loading, of the Durrães stone masonry arch bridge, a viaduct included in the Minho railway line connecting Porto to the Portuguese-Spanish border in the Minho river. Details and results of a broad experimental campaign on that bridge (using different in-situ testing techniques and in-lab procedures) can be found in Arêde et al. [4], which provided useful data concerning normal and shear response and stiffness of stone-to-stone joints in different weathering conditions.

3.3. Infill material characterization

3.3.1. In situ tests of infill material

As mentioned before, borehole dilatometer (BHD) tests were made in the Serra do Pilar church, as fully described in LNEC [14] and Almeida [1]. These tests provided mechanical deformability data relative to original walls' infill material of a 350 years old construction, at two different height level locations: the 1st test at 0.50 m and the 2nd test roughly at 11 m above the ground level

(near the windows' level), the former in the left buttress of the triumphal arch and the later in the immediately subsequent left side buttress. Tests were made in 1.80 m depth horizontal boreholes wherein the dilatometer was inserted into as shown in Fig. 14.

The dilatometer was developed at LNECLNEC (2000 for current use in rock mechanics testing. As illustrated in Fig. 15-a, it consists of a probe made of a stiff steel body with a rubber membrane in the central zone (0.60 m long) that allows applying hydrostatic pressure to 76 mm diameter boreholes' wall by means of water injection inside the rubber membrane. It is provided with four LVDT type transducers (with $1\ \mu\text{m}$ resolution), aligned in four directions separated by 45° , to obtain diametral displacements due to applied pressure that is measured by a digital pressure gauge (50 bar range and 0.1% full scale resolution) as shown Fig. 15-b.

The BHD was inserted up to the borehole full depth and displacements were recorded at approximately 1.50 m deep in the buttress thickness. After positioning, an initial pressure of 0.3 MPa was applied to ensure proper adjustment of the probe membrane to the borehole surface.

Test recordings allowed plotting applied pressure vs. diametral displacement in vertical and horizontal directions, as well as in 45° and 135° directions relative to the vertical. Loading-unloading-reloading cycles of pressure were applied up to about 1.3 MPa (see Fig. 16). As expected in this kind of soil type materials, the first loading up to a "virgin" stress state exhibits lower stiffness than subsequent reloading stages to the same stress level; this is evidenced in Fig. 16-a and -b, respectively, for the 1st and 2nd tests where the corresponding pressure vs. diametral displacement plots are shown for the vertical direction.

Similar diagrams were obtained for the three other directions, where lower deformations were recorded. For each load (pressure) stage, the average displacement of all four diametral directions



Fig. 14. Dilatometer tests' locations: a) 1st, near the ground; b) 2nd, about 11 m high.



Fig. 15. BHD tests: a) dilatometer probe; b) hydraulic pressure pump and control unit.

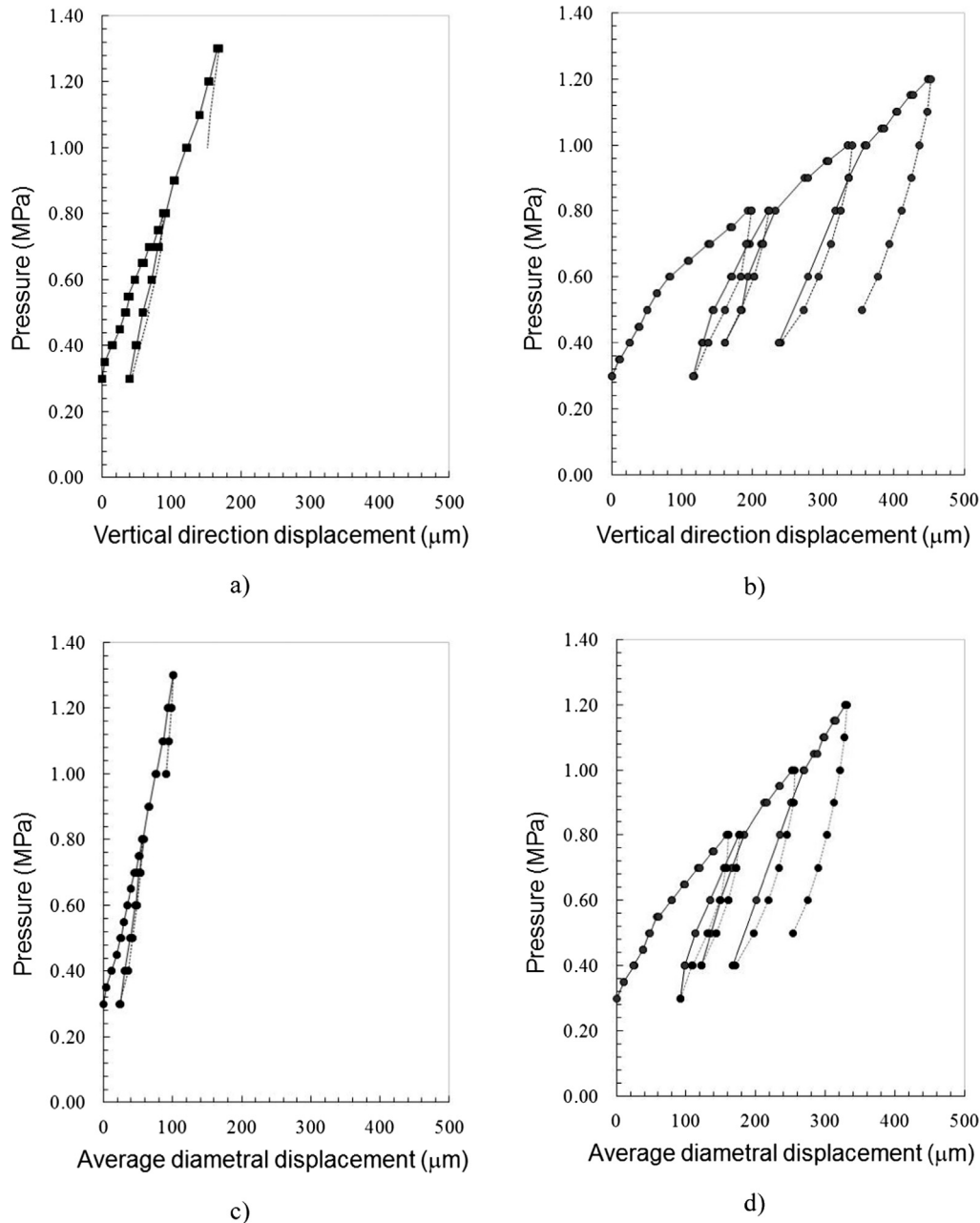


Fig. 16. Pressure vs. diametral displacement plots of BHD tests: a) 1st test and b) 2nd test for vertical direction response; c) 1st test and d) 2nd test for average response in the four directions.

was computed and the corresponding average response plot was obtained, as shown in Fig. 16-c and -d, respectively, for the 1st and 2nd tests. It is clear that, for the 1st test (lower level, near ground) a stiffer infill material was found than for the 2nd test (in the upper level), which is quite reasonable to accept as a plausible situation. This fact also justifies the reason why more cycles were made in the 2nd level; actually, the 1st test near the ground level was stopped earlier than expected (only one complete load-unload-reload cycle was achieved) due to failure of the rubber membrane, probably caused by its contact with a harsher conglomerate of sharp and stiff pieces of stone, mortar and voids.

Estimates of the “elastic” stiffness modulus can be obtained making use of Theory of Elasticity for an infinite length tube with internal diameter ϕ and infinite thickness, made of a homogeneous, isotropic and elastic material (with Young or elastic modulus E and Poisson ratio ν), submitted to an internal pressure p . The

corresponding displacement δ of the internal wall is therefore given by:

$$\delta = \frac{(1 + \nu)}{E} \cdot \phi \cdot p \quad (1)$$

The present case material is not homogeneous, isotropic and elastic, but still expression (1) can be used to derive values of equivalent elastic modulus E of a homogeneous, isotropic and elastic material having the same deformations obtained under the applied pressure. Without entering into much detail, considering 0.2 as an estimate of the Poisson ratio, average values of elastic modulus E for the 1st test were found about 0.9 GPa for first loading in “virgin” stress state ranges and about 1.3 GPa for unloading-reloading stages; for the 2nd test, the obtained values were around 0.3 GPa and 0.6 GPa, respectively for first loading and reloading conditions, therefore confirming quantitatively the above

mentioned lower material stiffness at the upper level of the tested buttress. Further details and exploitation of the results can be found in LNEC [14] and Almeida [1].

Several years after performing these tests, similar ones were made in two stone masonry arch bridges dating back to 1878/1879, both built in north of Portugal for the Minho railway line connecting Porto to the northern Spanish border. The bridges were object of broad experimental campaigns for structural and material characterization as described in Arêde et al. [4]. Concerning infill material of bridge piers, arches' intrados, boreholes were also made where pressuremeter tests were performed, in these cases using a Ménard type device. The testing principle is similar to that of BHD used in the Serra do Pilar church, the major difference being related to the borehole deformation measurement based on volume variation rather than displacement measurement through LVDTs. For these bridges, Ménard elastic modulus of the infill material ranged from about 0.25 GPa to 0.55 GPa, depending on the bridge and the test location. For completeness, it is mentioned that a similar application was made to study the material stiffness of buttresses of the S. Antonio church in Viana do Castelo, as described in Mesquita et al. [19] where much lower values (about 0.08 GPa) were found for the infill Ménard elastic modulus, probably due to the poor masonry that was actually present.

It is known that the Ménard elastic modulus E_M Baguelin et al. [5], Briaud [6] does not directly reflect the material Young modulus E due to non-uniform stress and strain fields around the Ménard probe. However, in the literature proposals can be found to estimate the Young modulus E from E_M by introducing a correction factor, the Ménard α factor, such that $E = E_M/\alpha$. According to Baguelin et al. [5], the α factor varies between 0.24 and 1, while Sedran et al. [23] suggest that the α factor depends on the compression stress normal to the probe. For the studied bridges' infill material where $E_M = 0.55$ GPa was obtained, the estimated vertical compression stress (thus normal to the probe) is slightly above 350 kPa, which, according to Sedran et al. [23], leads to an α factor around 0.33 and therefore to an estimated Young modulus of 1.65 GPa. Similarly, for the case of the S. Antonio church, the obtained values for E_M (around 0.08 GPa), associated with an estimate of slightly less than 200 kPa for vertical compressive stress, can be corrected by an α factor of 0.6, thus yielding an Young elastic modulus of 0.13 GPa. The so obtained values for Young modulus seem

compatible with the different types of infill materials present in the reported cases.

3.3.2. Lab tests of infill material

Samples of infill material of the Zameiro bridge (Fig. 2) were used to make oedometric tests as a first, more simple and not very expensive way of characterizing the deformability of such a loose and poor material collected in disturbed conditions. According to current geotechnical lab practices, the sample was laterally confined, with free drain at the top and bottom, and subjected to incremental axial load [10]. The values of oedometric modulus during the test ranged between 6.3 MPa and 23.7 MPa. In order to meet laterally unconfined conditions of bridge infill material, the elastic modulus (E) can be related to the oedometric modulus (E_{edom}) and the Poisson ratio (ν) through the expression (2).

$$E = E_{edom} \left(1 - \frac{2\nu^2}{1 - \nu} \right) \quad (2)$$

Considering 0.33 as a typical Poisson ratio for that kind of material it leads to $E = 0.67 E_{edom}$, for which E values ranged between 4.2 MPa and 15.2 MPa. Such values were adopted in numerical simulations of the Lagoncinha bridge (Fig. 3) since it has construction dates and features similar to the Zameiro bridge [7].

Taking advantage of full availability of the well graded granular material applied in the backfill of the Vila Fria bridge (Fig. 4), a broad characterization was made concerning its physical and mechanical properties, including parametric experimental studies to investigate the influence of different contents of binder (cement) foreseen to be present in the real construction. For this case, triaxial tests were carried out on samples of: i) pure granular material and ii) granular material with binder (7% of cement), as extensively described in [10]. Some of the corresponding results, in terms of deviatoric stresses ($\sigma_1 - \sigma_3$) vs. axial strain (ϵ_a) plots, are shown in Fig. 17 for three different consolidation stress levels (denoted as A, B and C, in increasing order), both for infill material samples without binder (samples type 1, Fig. 17-a) and with 7% cement (samples type 3, Fig. 17-b), where σ_3 is identified as the consolidation stress and σ_1 is the axial stress. The corresponding evolutions of volume variation (ΔV) recorded during the tests are plotted in Fig. 17-c) and -d), respectively.

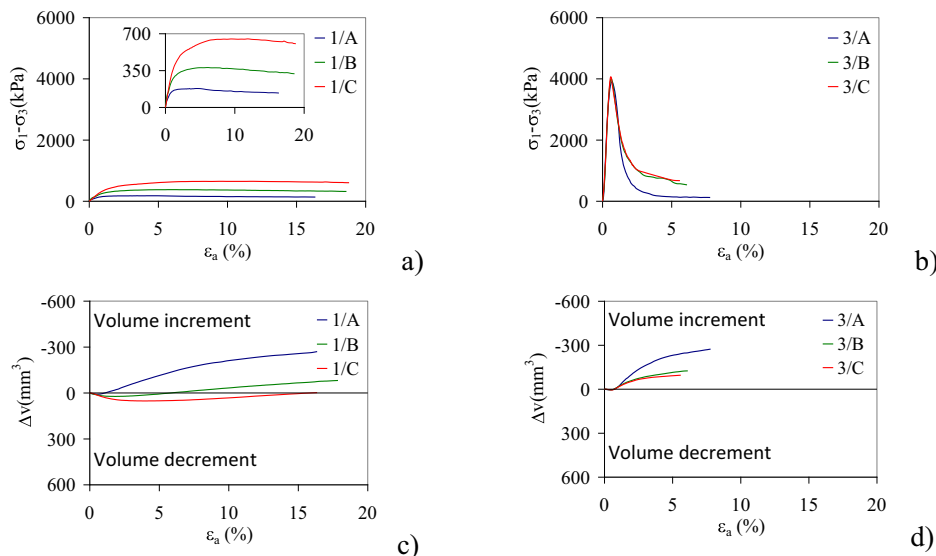


Fig. 17. Triaxial test results for infill material of Vila Fra bridge. Deviatoric stress ($\sigma_1 - \sigma_3$) vs. axial strain (ϵ_a) plots for samples, a) without binder, b) with 7% of cement and corresponding volume variation vs. axial strain plots, c) and d), respectively.

Table 2
Mechanical parameters of the infill material evaluated from triaxial tests.

Material parameter		Experimental values					
		Granular material			Granular material with 7% of cement		
Type of material:							
Sample ref.:		1/A	1/B	1/C	3/A	3/B	3/C
Consolidation stress (kPa):		30	80	150	10	50	80
$(\sigma_1 - \sigma_3)_{peak}$	(kPa)	180	379	651	3903	3996	4070
$(\varepsilon_a)_{peak}$	(%)	4.5	6.2	11.9	0.7	0.6	0.6
$(\sigma_1 - \sigma_3)_{residual}$	(kPa)	137	320	605	122	536	675
$(\varepsilon_a)_{residual}$	(%)	16.4	18.6	18.8	7.8	6.1	5.6
E_{60}	(MPa)	24.2	32.7	33.8	689.3	653.6	676.5
ψ	(°)	12.7	3.3	2.6	–	–	–

The pure granular material (Fig. 17-a) shows an initial phase of linear elastic behaviour, followed by hardening and a constant branch for the highest consolidation level (C); for lower consolidation stress levels smooth softening phases are observed, showing a slight strength peak due to dilatancy phenomena (Fig. 17-c). Quite different response is obtained for granular material with 7% of cement, showing almost linear response up to clear peak strength (see Fig. 17-b), followed by pronounced softening until a residual branch. Peak strength is not very influenced by the consolidation stress level and sample volume never decreases (by contrast with pure granular samples) due to the sample consistency granted by the cement addition.

For both cases, Mohr-Coulomb failure envelopes were possible to be drawn leading to friction angle about 42° and cohesion of 13 kPa for pure granular material, wherein cohesion is a consequence of imbrication between particles; for samples of granular material with cement, friction angle and cohesion were obtained as 33° and 1055 kPa, respectively, the latter clearly influenced by the cement bond effect.

From the triaxial tests' results shown in Fig. 17, several mechanical parameters were obtained for the two types of infill material used in the Vila Fria bridge as summarized in Table 2. Besides peak and residual deviatoric stress and axial strain values, the initial moduli of deformability, E_{60} , listed in Table 2 were evaluated from the curves $(\sigma_1 - \sigma_3, \varepsilon_a)$ using the least squares' method for deviatoric stress levels below 60% of the maximum values. The dilatancy angle, Ψ , also included in Table 2, was determined from the plots $(\Delta V, \varepsilon_a)$ shown in Fig. 17, following standard procedures of result analysis and processing of geotechnical triaxial tests.

3.4. General comments on results

The results obtained from the different experimental campaigns suggest a few comments described in the following.

Concerning joint behavior, from the Serra do Pilar (SP) church and Vila Fria (VF) bridge tests, dry joints in shear show reasonable agreement of values' ranges of mechanical parameters as well as shear stress-tangential displacement plots characterized by an initial linear elastic branch, followed by hardening and roughly constant stress plateau. In both cases the shear stiffness and strength depend on the normal stress, exhibiting Mohr-Coulomb envelopes with friction angles of the same magnitude order and null cohesion. By contrast, behaviour of dry joints in compression show notable differences of normal stiffness between SP and VF test results, the latter leading to lower values than the former. Apart from inherent material differences, the VF campaign of dry joints in compression involved much less specimens (just two), for which the corresponding results should be looked with caution. As for mortar joints in shear, same order of magnitude values were obtained for mechanical parameters from SP and VF test results. The shear stress-displacement curves also exhibit approximately

linear behavior up to peak stress, although, as expected and oppositely to dry joints, after which a residual plateau is reached by a softening branch (more pronounced in joints of the VF case). Similarly to dry joints, the shear stiffness and strength depend on the adopted normal stress for both SP and VF cases, leading to same order of magnitude of friction angles of Mohr-Coulomb envelopes with and non-zero cohesion conferred by the bonding effects of mortar. Oppositely, the normal stiffness of VF joint tests are much higher (about 10 times larger) than those of SP joints, clearly due to the stronger mortar (hydraulic lime based) used in the VF specimens.

As for infill material tests and results, in situ tests using borehole dilatometer in the SP church and Menard pressuremeter in railway bridges led to elastic moduli values of the same order of magnitude, from 0.25 to 1.3 GPa (depending on the location, material and first load/reload conditions). In both cases the material included large granite stone pieces, likely to yield significant stiffness, and compared well with triaxial lab tests on well-graded granular material provided with 7% of cement as binder. By contrast, both oedometric and triaxial lab tests made on granular rubble material, evidenced expectably much lower elastic moduli average values of about 0.01 to 0.03 GPa in the same order of magnitude of Menard pressuremeter elastic modulus obtained in-situ on a church buttress with very poor rubble stone infill material.

4. Final remarks

Material characterization of stone masonry historical structures still persists a challenging issue when realistic values of mechanical properties are sought to support the structural behaviour and safety assessment of ancient built heritage. It involves experiments on the constituent materials and their interfaces (i.e., stone blocks, interface dry or mortar joints and infill material), for which some techniques were reported in this paper in the context of their application for the characterization of stone masonry materials and components of a few cases representative of different types of historical structures.

Reported and used techniques are not new and essentially derive from geotechnical framework, namely rock and soil mechanics applications. In fact, for in-situ characterization of infill material of building thick walls or backfill of masonry bridges, both borehole dilatometer and Ménard pressuremeter tests were addressed, the corresponding results having been presented and discussed. Besides test results, these techniques involve tolerable hole drilling that allow visual inspection masonry constitution and collection of material samples of different masonry zones. Additionally, complementary lab tests (oedometric and triaxial) for infill material were reported as viable options when suitable samples are available. Also, appropriate core sampling of stone blocks and interface joints provide material to perform different

lab tests, of which joint shear and compression tests are highlighted as quite useful, yet very scarce for stone masonry heritage constructions, when numerical simulations are sought involving detailed discretization.

Beyond the presentation of testing techniques applications and results thereof obtained, the paper also aimed at drawing attention to the possibilities of using those techniques, often at a reasonable cost when the equipment is available, and to the important outcomes they can provide. Besides a few reference values of obtained mechanical properties, relevant but scarcely known bibliographic sources are referred where detailed information can be found relative to the reported techniques and the corresponding practical applications on historical structures.

Declaration of Competing Interest

None.

Acknowledgments

This work was financially supported by: Project POCI-01-0145-FEDER-007457 - CONSTRUCT - Institute of R&D In Structures and Construction funded by FEDER funds through COMPETE2020 - Programa Operacional Competitividade e Internacionalização (POCI) – and by national funds through FCT - Fundação para a Ciência e a Tecnologia. The authors thank the technicians of Laboratory for Earthquake and Structural Engineering (LESE) of FEUP, for their assistance with the experimental tests.

References

- [1] C. Almeida. *Análise do Comportamento da Igreja do Mosteiro da Serra do Pilar sob Acções Sísmicas*. (MSc thesis) Porto, FEUP. (in Portuguese, available at <http://nr.fe.up.pt/>), 2000.
- [2] C. Almeida, A. Arêde, A. Costa, *Seismic analysis of the Serra do pilar monastery church*, 12th European Conference on Earthquake Engineering, 2002. London.
- [3] A. Arêde, P. Costa, A. Costa, C. Costa, L. Noites, *Monitoring and Testing of a New Stone Masonry Arch Bridge in Vila Fria, Portugal Arch'07*, UM, Funchal, 2007.
- [4] A. Arêde, C. Costa, A.T. Gomes, J.E. Menezes, R. Silva, M. Morais, R. Gonçalves, *Experimental characterization of the mechanical behaviour of components and materials of stone masonry railway bridges*, *Constr. Build. Mater.* 153 (2017) 663–681.
- [5] F. Baguelin, J.F. Jezequel, D.H. Shields, *The Pressuremeter and Foundation Engineering*, TransTech Publications, 1978.
- [6] J.L. Briaud, *The Pressuremeter*, Balkema, 1992.
- [7] C. Costa. *Análise do comportamento da ponte da Lagoncinha sob a acção do tráfego rodoviário*. (MSc thesis). Porto, FEUP. (in Portuguese, available at <http://nr.fe.up.pt/>), (2002).
- [8] P. Costa. *Análise da Construção e do Comportamento duma Ponte de Pedra*. Tese de Mestrado, (MSc thesis). Porto, FEUP. (in Portuguese, available at <http://nr.fe.up.pt/>), 2007.
- [9] C. Costa, P. Costa, A. Arede, A. Costa, *Structural design, modelling, material testing and construction of a new stone masonry arch bridge in Vila Fria, Portugal*, in: 5th International Conference on Arch Bridges (ARCH'07), 2007, pp. 561–568.
- [10] C. Costa. *Análise numérica e experimental do comportamento estrutural de pontes em arco de alvenaria de pedra*. (PhD thesis). Porto, FEUP. (in Portuguese, available at <http://nr.fe.up.pt/>), 2009.
- [11] N. Domède, G. Pons, A. Sellier, Y. Fritih, *Mechanical behaviour of ancient masonry*, *Mater. Struct./Materiaux et Constr.* 42 (1) (2009) 123–133.
- [12] B. Ghiassi, D.V. Oliveira, P.B. Lourenço, G. Marcari, *Numerical study of the role of mortar joints in the bond behavior of FRP-strengthened masonry*, *Compos. Part B: Eng.* 46 (2013) 21–30.
- [13] ISCARSAH, *Recommendations for the analysis and restoration of historical structures*, International Committee on Analysis and Restoration of Structures of Architectural Heritage, ICOMOS, ISCARSAH, 2001.
- [14] LNEC. *Ensaio de Mecânica das Rochas na Igreja do Mosteiro da Serra do Pilar*. Technical Report. Laboratório Nacional de Engenharia Civil, Lisbon. (in Portuguese), 2000.
- [15] I. Lombillo, L. Villegas, J. Elices, *Minor destructive techniques applied to the mechanical characterization of historical rubble stone masonry structures*, *Struct. Survey* 28 (1) (2010) 53–70.
- [16] I. Lombillo, L. Villegas, E. Fodde, C. Thomas, *In situ mechanical investigation of rammed earth: calibration of minor destructive testing*, *Constr. Build. Mater.* 51 (2014) 451–460.
- [17] G. Macchi, G. Ruggeri, M. Eusebio, M. Moncecchi, *Structural assessment of the leaning tower of pisa*, IABSE Symposium, *Structural Preservation of the Architectural Heritage*, 1993. Rome.
- [18] C. Mazzotti, E. Sassoni, G. Pagliai, *Determination of shear strength of historic masonries by moderately destructive testing of masonry cores*, *Constr. Build. Mater.* 54 (2014) 421–431.
- [19] E. Mesquita, A. Arêde, R. Silva, P. Rocha, A. Gomes, N. Pinto, P. Antunes, H. Varum, *Structural health monitoring of the retrofitting process, characterization and reliability analysis of a masonry heritage construction*, *J. Civ. Struct. Health Monit.* 7 (3) (2017) 405–428.
- [20] J. Milosevic, A. Sousa Gago, M. Lopes, R. Bento, *Experimental assessment of shear strength parameters on rubble stone masonry specimens*, *Constr. Build. Mater.* 47 (2013) 1372–1380.
- [21] G.S. Pavan, K.S. Nanjunda Rao, *Behavior of brick-mortar interfaces in FRP-strengthened masonry assemblages under normal loading and shear loading*, *J. Mater. Civ. Eng.* 28 (2) (2016).
- [22] L. Pelà, P. Roca, A. Benedetti, *Mechanical characterization of historical masonry by core drilling and testing of cylindrical samples*, *Int. J. Archit. Heritage* 10 (2–3) (2016) 360–374.
- [23] G. Sedran, R.A. Failmezger, A. Drevininkas, *Relationship between menard EM and Young's E moduli for cohesionless soils*, 18th International Conference on Soil Mechanics and Geotechnical Engineering, 2013. Paris.
- [24] A. Rahman, T. Ueda, *Experimental investigation and numerical modeling of peak shear stress of brick masonry mortar joint under compression*, *J. Mater. Civ. Eng.* 26 (9) (2014).
- [25] C. Sandoval, O. Arnau, *Experimental characterization and detailed micro-modeling of multi-perforated clay brick masonry structural response*, *Mater. Struct./Materiaux et Constr.* 50 (1) (2017).
- [26] G. Vasconcelos, P.B. Lourenço, *Experimental characterization of stone masonry in shear and compression*, *Constr. Build. Mater.* 23 (11) (2009) 3337–3345.